NIH Public Access
Author Manuscript
Stem Cells. Author manuscript; available in PMC 2012 April 16.

Published in final edited form as:
Stem Cells. 2009 May ; 27(5): 993–1005. doi:10.1002/stem.29.

Functional Evidence that the Self-Renewal Gene *NANOG* Regulates Human Tumor Development

Collene R. Jeter[1], **Mark Badeaux**[1], **Grace Choy**[1], **Dhyan Chandra**[1], **Lubna Patrawala**[1], **Can Liu**[1], **Tammy Calhoun-Davis**[1], **Holm Zaehres**[2], **George Q. Daley**[2], and **Dean G. Tang**[1]

[1]Department of Carcinogenesis, University of Texas M.D Anderson Cancer Center, Science Park-Research Division, Smithville, Texas, USA

[2]Harvard Stem Cell Institute and Harvard Medical School, Children's Hospital, Boston, Massachusetts, USA

Abstract

Tumor development has long been known to resemble abnormal embryogenesis. The embryonic stem cell (ESC) self-renewal gene *NANOG* is purportedly expressed by some epithelial cancer cells but a causal role in tumor development has remained unclear. Here, we provide compelling evidence that cultured cancer cells, as well as xenograft- and human primary prostate cancer cells (HPCa) express a *functional* variant of Nanog. *NANOG* mRNA in cancer cells is derived predominantly from a retrogene locus termed *NANOGP8*. NANOG protein is detectable in the nucleus of cancer cells and is expressed higher in patient prostate tumors than matched benign tissues. *NANOGP8* mRNA and/or NANOG protein levels are enriched in putative cancer stem/progenitor cell populations. Importantly, extensive loss-of-function analysis reveals that RNAi-mediated Nanog knockdown inhibits tumor development, establishing a functional significance for Nanog expression in cancer cells. Nanog-shRNA transduced cancer cells exhibit decreased long-term clonal and clonogenic growth, reduced proliferation and, in some cases, altered differentiation. Thus, our results demonstrate that Nanog, a cell-fate regulatory molecule known to be important for ESC self-renewal, also plays a novel role in tumor development.

Keywords

Nanog; tumor development; tumor-initiating cell; cancer stem cell; self-renewal

INTRODUCTION

Cancer cells and embryonic stem cells (ESCs) share many key biological properties. A cardinal trait possessed by both cell types is extensive proliferative potential essential to embryogenesis and tumor development. Pluripotency is also fundamental to ESCs and gives rise to the myriad of differentiated daughter cells present in the mature embryo. Similarly, multipotent cancer cells seem to exist that may recapitulate the tumor of origin upon transplantation [1]. Such tumor-initiating cells, often termed cancer stem cells (CSCs), contribute to tumor homeostasis; however, the molecular mechanisms that underlie the perpetual growth and plasticity of CSCs have scarcely been elucidated.

Correspondence: Dean Tang, M.D., Ph.D., Department of Carcinogenesis, University of Texas M.D Anderson Cancer Center, Science Park-Research Division, Smithville, TX 78957, USA. Tel: (512) 237-9575; Fax: (512) 237-2475; dtang@mdanderson.org.

Author contributions: C.J.: conception and design, collection and assembly of data, data analysis and interpretation, manuscript writing; M.B., G.C., D.C., L.P., C.L., T.C.: collection and assembly of data; H.Z., G.D.: provision of study material; D.T.: conception and design, data analysis and interpretation, manuscript writing, final approval of manuscript.

NIH-PA Author Manuscript
NIH-PA Author Manuscript
NIH-PA Author Manuscript

NIH-PA Author Manuscript

NIH-PA Author Manuscript

NIH-PA Author Manuscript

Self-renewal is essential to the maintenance of stem cell (SC) populations, and cancer cells have also been evidenced to renew as demonstrated by secondary (2^o) growth assays, including serial tumor transplantation and sphere-formation assays. Remarkably, single-cell derived colon cancer spheres and tumors comprised of a mixture of cell lineages have recently been shown to arise from a subset of cancer cells expressing CSC markers [2]. Thus, in principle, the molecular mechanisms that mediate ESC self-renewal may also operate in renewing cancer cells. Transcription factors represent critical molecular switches regulating SC fate. Three transcription factors, Sox2, Oct3/4 (Oct4), and Nanog [3, 4] form a core regulatory network that coordinately determines ESC self-renewal and differentiation [5, 6] These ESC self-renewal molecules may conceptually also contribute to tumorigenesis. In support, Nanog is expressed not only in germ cell tumors [7] but also reported to be expressed in other tumors including carcinomas of the breast [8, 9], cervix [10], oral cavity [11], kidney [12], and ovary [13]. Also, ectopic expression of *Oct4* in transgenic mice is sufficient to induce hyperplasia and dysplasia in the epidermis and intestinal crypt [14] and Nanog overexpression promotes proliferation and transformation of NIH3T3 cells [15].

Cancer cells expressing *Oct4* mRNA are frequently implied to mark putative CSCs [e.g., 13, 16]. A potential danger in making such a connection is that *Oct4* has multiple copies of processed but non-functional pseudogenes [17], which can mimic proper mRNA and generate false-positive RT-PCR products [18]. In support, some 'Oct4-positive' cancer cell lines were later found to lack credible expression of Oct4 mRNA and protein [19]. Genetic analysis also does not support a significant role for *Oct4* in regulating normal mouse somatic SCs [20]. On the other hand, recent loss-of-function studies demonstrate that Oct4 is an important mediator of some cancer cell phenotypes including survival and invasion [21, 22].

Like OCT4, NANOG has also been reported in some non-germ cell tumors (above) and *NANOG* also possesses multiple pseudogenes (see below). However, comprehensive and systematic studies of *NANOG* mRNA and NANOG protein expression in human tumor cells are still lacking. More importantly, it remains unclear whether the expression of NANOG in cancer cells plays a causal role in tumor development. In this study, we set out to test the hypothesis that the ESC self-renewal molecule NANOG contributes to cancer cell clonogenic or tumorigenic growth properties. Herein, we provide convincing evidence that tumor cells in vitro and in vivo express a retrotransposed *NANOG* gene and that NANOG protein is functionally important in regulating human tumor development.

MATERIALS AND METHODS

Xenografts, Tumor Dissociation, Flow-Activated Cell Sorting (FACS) and Transplantation

Cells, xenografts, and basic experimental procedures for tumor dissociation, FACS, in vitro characterization and subcutaneous (s.c.) transplantation were detailed elsewhere [23–25]. PCa samples were obtained at radical prostatectomy with patients' consent by the IRB-approved guidelines. Minced tumor tissues were subject to enzymatic digestion (type I collagenase, 50 U/ml DNase, 12 h), followed by trypsin digestion and discontinuous Percoll gradient purification. Primary (1^o) HPCa cells were recombined with rat urogenital sinus mesenchyme (rUGSM) in collagen drops and transplanted under the renal capsule as previously described [26] (see Supplementary Experimental Procedures [SEP] for details).

RT-PCR and Quantitative Real-time RT-PCR

Total RNA was extracted from cancer cells or hESC (cell line WA09/H9, cultured as previously described [27]) using an RNeasy RNA-purification kit (Qiagen, Valencia, CA). PCR primers are indicated in table S1. Real-time PCR was performed using an ABI Prism

NIH-PA Author Manuscript

NIH-PA Author Manuscript

NIH-PA Author Manuscript

7900HT and the TaqMan system (ABI), and the Nanog primers and probes previously described [27] (see SEP).

Cloning and Characterization of Cancer Cell Derived NANOG

NANOGP8 cDNA was amplified by PCR using LDF1/LDR1 primers and cloned in pCR2.1 (Invitrogen). Sequencing was performed using the ABI Prism 3130×l Genetic Analyzer. The EcoR I/Sal I fragments containing the *NANOG* coding sequence were subcloned into pET-28b(+), and His-tagged NANOG proteins were purified from transformed bacteria per manufacturer (Qiagen). Samples were run on 12% SDS-PAGE and proteins were transferred to nitrocellulose membrane and probed as described. Tryptic digests were analyzed using a 4700 Proteomics Analyzer MALDI-TOF/TOF (Applied Biosystems, Foster City, CA).

Immunofluorescence (IF) and Immunohistochemistry (IHC) Staining

Fluorescence microscopy basic procedures have been described [23–25] (see SEP; antibodies in table S2). IF detection of NANOG required permeabilization and denaturation pretreatment (0.5% TritonX100, 0.25% sodium dodecyl sulfate). For IHC, formalin fixed, paraffin-embedded tissue sections were deparaffinized and hydrated. Endogenous peroxidase activity was blocked (3% H_2O_2) and antigen retrieval was performed (10 mM citrate buffer; pH 6.0). After Biocare Blocking Reagent (Biocare, Concord, CA) 1^0 antibodies (NANOG antibodies 1:100; 2 h), were followed by biotinylated 2^0 antibody, streptavidin-conjugated horseradish peroxidase and DAB development.

Lentiviral Production and Transduction

Lentiviruses containing the pLL3.7, LL-Luc, Oct4-shRNA and Nanog-shRNA [27] or the TRC-shRNA (TRCN000004887) or pGIPZ-Nanog shRNA vectors (Open Biosystems, Huntsville, AL) were produced in 293FT packaging cells as previously described [27] (see SEP).

Phenotype ‘Rescue’ Experiments

Non-directional cloning of *NANOGP8* into pPyCAG [3] was performed by ligating the XhoI/SalI fragment of pCR2.1-HPCa5-Nanog into the XhoI site of pPyCAG. Cells were infected with lentivirus 24 h prior to transfection, replated on coverslips and subject to the BrdU proliferation assay (see SEP).

RESULTS

Various cancer cells express *NANOG* mRNA

To assess the mRNA expression of *NANOG*, we initially employed two pairs of primers: the F1/R1 pair that spans the intron 3 of human *NANOG* (or *NANOG*1) and the LDF1/LDR1 pair that amplifies the full-length *NANOG*1 mRNA (Fig. 1A; also see table S1 and fig. S1). The results revealed the expected 312-bp F1/R1 *NANOG* band (fig. S2A-C) as well as the ~1-kb LDF1/LDR1 *NANOG* band (Fig. 1B-C; fig. S2D) in cultured prostate cancer (PCa; Du145, PC3, PPC-1, and LNCaP), breast cancer (MCF7 and MDA-MB435), and colon cancer (Colo320), among others. Importantly, cancer cells freshly purified from xenograft tumors (LAPC4 and LAPC9; fig. S2A) as well as primary human PCa (HPCa; Fig. 1C; fig. S2C-D) samples also showed *NANOG* expression. As expected, full-length *NANOG* mRNA was detected in embryonal carcinoma N-tera cells (Fig. 1B). Similar to *NANOG*, RT-PCR for *OCT4* using a pair of primers that span introns 3 and 4 detected the expected 573-bp band in all cancer cells examined (fig. S2A-D). By contrast, *SOX2* mRNA was detected only in a fraction of the samples, with cultured PCa cells notably lacking *SOX2* mRNA (fig. S2A-B).

NIH-PA Author Manuscript

NIH-PA Author Manuscript

NIH-PA Author Manuscript

In order to quantify the relative mRNA expression level of *NANOG* in cancer cells, we performed real-time quantitative RT-PCR (qRT-PCR) analysis. *NANOG* mRNA in LAPC4, LAPC9 and Du145 xenograft tumor cells represented only approximately 1.4%, 0.5%, and 0.45%, respectively, of the *NANOG* mRNA levels in undifferentiated hESCs. Primary HPCa cells freshly purified from patient tumors expressed higher relative levels of *NANOG* mRNA, at 4.5%, 12.1% and 7.0% for HPCa5, HPCa6 and HPCa7, respectively.

Cancer cell *NANOG* mRNA is derived from a transcribed pseudogene, *NANOGP8*

Human *NANOG1* gene (gi 13376297), the gene commonly referred to as *NANOG* and localized on chromosome 12, has four exons and three introns with a 915-bp ORF (Fig. 1A). Alternate loci that could potentially encode *NANOG* mRNA variants include a tandemly duplicated gene *NANOG2* (also called *NANOGP1* with a 696-bp ORF; [28]), and nine retrotransposed genes, eight of which have defects (e.g. deletions, frameshifts, stop codons, etc.). Interestingly, one *NANOG* pseudogene (*NANOGP8* or *PN8* located on chromosome 15; gi 47777342) is free of structural defects and has the potential to be functionally expressed [29].

The F1/R1 primers should amplify a 312-bp *NANOG1* or *NANOGP8* fragment or a 255-bp *NANOG2* product (fig. S1; table S1). In our experiments, we only detected the 312-bp band (fig. S2A-C), suggesting that *NANOG*2 is not expressed in cancer cells. In support, RT-PCR using primers designed to amplify full-length *NANOG*2 (LDF2/LDR1; fig. S1) did not generate *NANOG2*-specific product in cancer cells (not shown). To distinguish whether cancer cells express *NANOG1* and/or *NANOGP8* mRNA, we cloned the LDF1/LDR1 PCR products from multiple cancer cells. Sequencing analyses revealed that N-tera cells expressed *NANOG1* but not *NANOGP8* mRNA whereas all other cancer cells showed 5 of 6 nucleotide (nt) differences specific to *NANOGP8* [29]; (Fig. 1D, marked in blue). Among the 5 conserved nt changes in *NANOGP8* (relative to *NANOG1*; [29]), only one (nt759) results in aa change (Q253H; Fig. 1D, indicated in red) although some cancer cells also showed other non-conserved nt changes that could also result in aa changes (e.g., L61P for HPCa6, Fig. 1D). The published nt sequence for *NANOGP8* may contain a sequencing error (or polymorphism) at nt 47 (Fig. 1D). No stop codons or frame shifts were detected in any of the cancer cell *NANOG* transcripts.

To lend further support to *NANOGP8* being the major *NANOG* transcript in cancer cells, we took advantage of a small deleted region in the 3'-UTR of *NANOGP8* (fig. S1) and designed primers that can discriminate between *NANOG1* and *NANOGP8*. As shown in Fig. 1E, the same forward primer (F2) together with either a downstream 'universal' *NANOG* reverse primer (R3) or an upstream *NANOG1*-specific reverse primer (R2) (table S1; fig. S1) both generated a robust PCR product of the correct size in hESCs. In contrast, in cancer cell samples the F2/R2 primer pair failed to generate the 335-bp *NANOG1* band (Fig. 1E, top) but the 'universal' F2/R3 primer pair detected the expected 446-bp *NANOGP8* in cancer cells, and the 467-bp *NANOG1* in hESCs (Fig. 1E, bottom, arrow). Interestingly, smaller amplicons were also detected (Fig. 1E, bottom, asterisks), perhaps indicating splicing variations in the 3'UTR of *NANOG1* and *NANOGP8*.

The above results suggest that cancer cells preferentially express *NANOG* from the *NANOGP8* locus rather than *NANOG1*, which might be silenced in cancer cells as in differentiating ESCs [30]. Indeed, treatment of PC3 cells with the histone deacetylase inhibitor trichostatin A (TSA) but not the DNA methyltransferase inhibitor 5'-aza-2'-deoxycytidine (Aza) upregulated *NANOG1* mRNA (Fig. 1F). In contrast, the mRNA of cyclin-dependent kinase inhibitor p16, known to be silenced in PCa cells due to promoter hypermethylation, was upregulated by Aza treatment (Fig. 1F). Together, these results suggest that cancer cell *NANOG* transcript is largely derived from *NANOGP8*.

NIH-PA Author Manuscript

NIH-PA Author Manuscript

NIH-PA Author Manuscript

NANOG protein expression in cancer cells and enrichment in CD44^{hi} PCa and MCF7 side population (SP) cells

Human (and mouse) Nanog has 305 aa predicted to encode a ~35 kD protein [4]. However, Nanog proteins of 35 kD to ~50 kD have been detected on Western blotting in ESCs, EC, germ cell tumors and some cancer cells [e.g., 4, 31]. *NANOGP8* mRNA is essentially identical to *NANOG* mRNA and is thus predicted to encode a nearly identical (>99%) NANOG protein. To determine whether *NANOGP8* mRNA in cancer cells could potentially encode a functional protein recognized by anti-NANOG antibodies, we cloned the LDF1/LDR1 *NANOGP8* cDNAs into His-tagged bacterial expression plasmids. Western blotting showed that the recombinant proteins derived from the cancer cell *NANOGP8* cDNAs were all recognized specifically by an affinity-purified monoclonal anti-Nanog antibody (i.e., eBio mAb; table S2) as a ~42 kD protein (Fig. 1G). The identity of the 42 kD protein bands was subsequently verified to be NANOG by peptide sequencing (Fig. 1H). For the sake of clarity, and because of the high degree of aa identity between the predicted polypeptides derived from the *NANOG1* locus and the *NANOGP8* locus, we shall simply refer to the corresponding protein in cancer cells as NANOG in most of the foregoing discussions.

The eBio mAb to NANOG also detected a ~42 kD band in PC3, LNCaP, MCF7, Colo320 and WM562 cells using either whole cell lysate (WCL; Fig. 1I) or nuclear extracts (NE; Fig. 1J); similar results were obtained using another affinity-purified polyclonal antibody (Kamiya pAb; table S2; data not shown). The eBio mAb also detected a prominent upper band migrating at ~47 kD (Fig. 1I-J). Both of the bands detected by the eBio anti-NANOG antibody appear specific, as Nanog-shRNA knocked down both bands in LAPC4 xenograft cells (not shown) and completely eliminated the two bands in LNCaP cells (see Fig. 4D, below).

Indirect immunofluorescence (IF) staining using either Ab with Triton permeabilization and biotin amplification (see Methods) readily detected NANOG in undifferentiated ‘islands’ of N-tera cells (fig. S3A). Using identical staining protocol, we only detected nuclear NANOG in a small percentage (<1%) of cultured MCF7, LNCaP, and PC3 cells (fig. S3A) as well as PCa cells freshly purified from patient tumors (fig. S3B). In some cells perinuclear (e.g., in MCF7) or cytoplasmic (e.g., in LNCaP and HPCa11) staining was also observed (fig. S3).

Reports of Nanog functioning in higher order protein-protein complexes [6, 32] prompted us to develop a novel IF protocol that incorporated a denaturation step (see Methods). Using this modified protocol, we found that the Kamiya pAb stained NANOG in the nucleus and perinuclear region of Du145 cells (fig. S4). The staining was abrogated by preincubating the Ab with recombinant NANOGP8 (fig. S4j-l) and was largely absent in Du145 cells infected with Nanog-shRNA (fig. S4p-r). Comparing the two staining protocols in N-tera and LNCaP cells with yet another, newly available anti-Nanog antibody (i.e., the Santa Cruz [SC] pAb; table S2) similarly revealed that, although NANOG protein was readily detected in N-tera cells without denaturation, specific nuclear NANOG staining in LNCaP cells was observed only after denaturation (fig. S5A). Importantly, the SC pAb, detected predominantly nuclear NANOG in other cancer cells including Du145 and PC3 (Fig. 2A; fig. S5B) and the results were confirmed by confocal microscopy (Fig. 2B). A gradient of NANOG staining was apparent with some cells largely negative (Fig. 2Af, circled). Interestingly, we consistently observed higher levels of NANOG in dividing cancer cells (Fig. 2Af and i, fig. S4j-i, fig. S5g-i, m-o, p-r; arrows).

Using a sensitive polymer-based IHC system (see Methods), we detected nuclear NANOG protein in scattered or clustered tumor cells in MCF7, Du145 and LAPC4 xenografts (Fig. 2C; data not shown). Using the Kamiya Ab, we analyzed NANOG expression in situ in 24 primary HPCa samples and, in 14 cases, compared its expression with the corresponding

NIH-PA Author Manuscript

NIH-PA Author Manuscript

NIH-PA Author Manuscript

benign prostate tissues. This small-scale IHC study (Fig. 2D; fig. S6; table S3) revealed several important points. *First*, NANOG-positive cells were detected in all HPCa samples but, like the histopathology of HPCa, NANOG expression was heterogeneous at both inter- and intratumoral levels. *Second*, in Gleason 6 and 7 tumor glands, NANOG-expressing cells were observed in both luminal and basal (like) cells. *Third*, in the majority of cases, NANOG was distinctly nuclear; however, cytoplasmic staining was observed in a few cases. *Fourth*, significantly, comparison of NANOG expression in tumors (T) and matched benign (Bn) tissues revealed more NANOG-positive cells in the tumors (Fig. 2Dd-f; table S3; fig. S6). IHC staining using the SC pAb demonstrated similar staining patterns (fig. S7) with some dysplastic, undifferentiated tumor areas showing large numbers of nuclear NANOG-positive cells (fig. S7A and D).

To test the possibility that NANOG-expressing cells might be enriched in potential cancer stem/progenitor cell populations, we carried out double IF staining for NANOG and CD44, which marks PCa stem/progenitor cells [24, 25, 33]. The results revealed that the $CD44^{hi}$ Du145 (Fig. 2E) and PC3 (fig. S8) cells appeared to express higher levels of NANOG. CD44 showed typical plasma membrane and cytoplasmic staining whereas NANOG showed mainly nuclear/perinuclear with some cytoplasmic localization (Fig. 2E; fig. S8). qRT-PCR analysis of purified Du145 xenograft cells revealed a 10-fold enrichment of *NANOGP8* mRNA in the $CD44^{hi}$ compared to bulk cells (not shown). We further purified, from HPCa38 and HPCa39 tumors, respectively, the $CD44^{+}CD133^{+}$ and $CD133^{+}$ cells, previously reported to mark primary prostate CSCs [34], and qRT-PCR revealed ~5 fold higher *NANOGP8* mRNAs in both populations than their corresponding negative cell populations (Fig. 2F). Moreover, we frequently observed an inverse relationship between NANOG and the prostate differentiation marker AR (e.g., fig. S8Bc-d; fig. S8Cb-c). Finally, we also observed ~4-fold higher *NANOGP8* mRNA levels in the MCF7 side population (SP) cells (Fig. 2G), which we previously had shown to express higher levels of β-*CATENIN* and *NOTCH-1* mRNAs, and be enriched in stem-like tumor-initiating cells [23].

RNAi-mediated Nanog knockdown inhibits tumor development

The preceding experiments provide convincing evidence for NANOG expression in cancer cells in vitro and in vivo. To determine its potential biological functions in cancer cells, we carried out pilot loss-of-function experiments using siRNA pools. Nanog-siRNA inhibited the clonogenic growth of both LNCaP and MCF7 cells relative to control and Sox2-siRNA (fig. S2-E-H), despite SOX2 expression at the protein level in MCF7 cells (fig. S9). To more fully investigate the functions of NANOG in tumor development, we made extensive use of lentiviral vectors encoding specific shRNAs. To ensure the specificity of Nanog knockdown we utilized three different vectors targeting different regions of *NANOG1/NANOGP8* (Fig. 1A; Table 1), including the pLL3.7-based lentiviral vector targeting the 3'-UTR and previously used to knockdown *NANOG1* in ESCs (Nanog-shRNA; [27]); an untagged Nanog-shRNA vector obtained from The RNAi Consortium (TRC-shRNA) targeting the coding region of *NANOG*; and pGIPZ-Nanog (Open Biosystems), targeting the 3'-UTR. Several control vectors included empty vector pLL3.7, a control vector targeting luciferase (LL-LUC), and an shRNA expressing/non-silencing control pGIPZ vector (pGIPZ-control).

PCa (Du145, LAPC4, LAPC9, and HPCa18), breast cancer (MCF7), and colon cancer (Colo320) cells were infected with various lentiviral vectors at an MOI (multiplicity of infection) of 10–20 and then used in tumor experiments. Infected cells (exhibiting decreased *NANOG* mRNA levels; fig. S10) were either injected subcutaneously (s.c.) in Matrigel into NOD/SCID mice or transplanted in collagen drops under the renal capsule (for HPCa cells). As summarized in Table 1 and Fig. 3 the three Nanog-shRNA constructs consistently inhibited tumor development of prostate, breast and colon cancer cells with smaller and/or fewer tumors. For example, in Du145 PCa cells, two different Nanog-shRNA constructs

NIH-PA Author Manuscript

NIH-PA Author Manuscript

NIH-PA Author Manuscript

exhibited similar tumor-inhibitory effects, even relative to the shRNA expressing, non-targeting control (pGIPZ-control; Table 1; Fig. 3Aa). Nanog-shRNA tumors that did arise exhibited reduced GFP (Fig. 3Bb) so we utilized FACS to sort out the GFP^{bright} Du145 cells from their respective first-generation tumors and carried out secondary (2^o) transplantation experiments. The 2^o GFP^{bright} Nanog-shRNA Du145 cells generated significantly smaller tumors compared with GFP^{bright} LL3.7 cells (Fig. 3Ab). Similar tumor inhibitory effects were obtained in LAPC9 and LAPC4 PCa xenograft tumor models (Fig. 3Ba; Table 1).

To determine whether NANOG is also potentially involved in 1^0 HPCa tumorigenicity, freshly purified HPCa18 cells were transduced and recombined 10,000 cells each with an equal number of rUGSM cells, and transplanted under the renal capsule of male NOD/SCID mice. This pilot experiment showed that LL3.7-infected HPCa18 cells formed the largest outgrowths (2/2) whereas the Oct4-shRNA infected cells generated smaller outgrowths (2/2) and the Nanog-shRNA-infected cells did not regenerate any outgrowth (0/2) (Fig. 3C-D; Table 1). Histologically, the LL3.7-infected HPCa18 cells reconstituted the full spectrum of pathological lesions present in the patient tumor, consisting of benign glands and PIN (prostate intraepithelial neoplasia)-like lesions (Fig. 3Da), and undifferentiated tumor cells with highly pleiomorphic nuclei (Fig. 3Db). The outgrowth was derived from human cells as evidenced by staining for human-specific mitochondria (Fig. 3Dc).

Nanog knockdown likewise inhibited MCF7 and Colo320 tumor development (Table 1). As shown in Fig. 3E, both Nanog-shRNA and TRC-shRNA significantly inhibited MCF7 tumor development, and, although Oct4-shRNA demonstrated a modest inhibitory effect on MCF7 tumor development, the effect was not statistically significant (Fig. 3Ea-b). Similarly, knocking down Nanog consistently inhibited Colo320 tumor development whereas Oct4-shRNA demonstrated inconsistent effects (Table 1; Fig. 3Fa-b). As observed for Du145, LAPC9 and LAPC4 cells, Nanog-shRNA transduced Colo320 tumors that did arise had mostly lost GFP (Fig. 3Fc), suggesting that these tumors likely regenerated from rare tumor cells that were uninfected or alternatively, from tumor cells that had lost shRNA (and corresponding GFP) expression.

Nanog shRNA-transduced cancer cells exhibit decreased proliferation and clonal/clonogenic potentials

Next, we explored the molecular mechanisms underlying the tumor-inhibitory effects of Nanog knockdown. Nanog-shRNA significantly restricted the clonal expansion of PC3 cells such that cells infected with Nanog-shRNA formed only sparse clones whereas cells infected with LL3.7 became confluent (Fig. 4A). Oct4-shRNA showed no apparent effect (Fig. 4A, fig. S11) although both Nanog-shRNA and Oct4-shRNA partially downregulated their respective target mRNAs in PC3 cells (fig. S10). Upon serial passaging, Nanog-shRNA significantly inhibited the cumulative population doublings (PDs) (Fig. 4Ba), and in clonal analysis, Nanog-shRNA and TRC-shRNA treated cells showed lower cloning efficiency (CE) and smaller clone sizes (Fig. 4Bb-c; fig. S11). In 2^o clonal analysis, cells initially infected with the control or Oct4-shRNA lentiviruses showed enhanced CE whereas the Nanog-shRNA infected PC3 cells exhibited lower CE (Fig. 4Bd).

Nanog-shRNA and TRC-shRNA completely abrogated NANOG protein expression (Fig. 4D), coincident with inhibited clonal expansion of LNCaP cells (Fig. 4Ca-c; fig. S12). Nanog-shRNA also inhibited the clonogenicity of LNCaP cells sufficiently to ablate the formation of 2^o spheres (Fig. 4Cd). Nanog-shRNA similarly inhibited the clonal (fig. S12A-B) and clonogenic (not shown) potentials of another PCa cell line, Du145. The apparent growth inhibitory effect of Nanog knockdown was not associated with increased cell death as assessed by morphology, Annexin V labeling, and nuclear DAPI staining (data not

NIH-PA Author Manuscript

NIH-PA Author Manuscript

NIH-PA Author Manuscript

shown). Rather, cell proliferation was partially inhibited as assessed by BrdU incorporation assays (fig. S12C-D).

To determine whether Nanog regulates in vitro growth properties of patient tumor cells, we purified HPCa22 cells from prostatectomy specimen and carried out clonal and clonogenic assays. As shown in Fig. 5A-B and table S4 both Nanog-shRNAs strongly inhibited the clonal growth of primary HPCa22 cells. Oct4-shRNA marginally inhibited the clonal development of HPCa22 cells but the inhibitory effect was not statistically significant (table S4). LL3.7-infected HPCa22 cells formed tight holoclones (large compact clones previously shown to contain self-renewing cancer cells [35]) whereas cells infected with the Nanog/TRC-shRNA generally formed small paraclones composed of scattered, large cells (Fig. 5A-C). When the clonal cultures were passaged, LL3.7-infected cells proliferated extensively and formed a typical 'cobblestone'-like epithelial sheet whereas HPCa22 cells infected with Nanog-shRNA became large and flat, and turned senescent evidenced by positive SA-βgal staining (Fig. 5C-D). Similar clonal experiments with HPCa25 and HPCa37 also revealed inhibitory effects of Nanog shRNAs (table S4).

Nanog-shRNAs also inhibited the anchorage-independent growth of HPCa22 cells. Although LL3.7-infected HPCa22 cells formed numerous large/solid spheres, HPCa22 cells infected with either Nanog shRNA formed fewer and smaller spheres (Fig. 5E) exhibiting a differentiated morphology with a hollow core (Fig. 5E-F). Interestingly, CD44 appeared downregulated in Nanog-shRNA spheres (Fig. 5F). When the 1^{o} spheres were dissociated and replated, the LL3.7, Oct4, Nanog, and TRC-shRNA infected cells showed a 2^{o} sphere-forming capacity of 54 ± 12, 22 ± 3.8, 16 ± 3.2, and 0, respectively. Similarly, LAPC4 xenograft cells transduced with Nanog-shRNA constructs also demonstrated reduced sphere-forming potential (fig. S13).

Nanog-shRNA also inhibited MCF7 breast cancer cell clonal expansion (Fig. 6A) clearly associated with an inhibition of proliferation (Fig. 6B-C). Following a 4-h BrdU pulse, ~49% of the LL3.7 or Oct4-shRNA transduced MCF7 cells incorporated BrdU whereas only ~22% of the Nanog shRNA-infected MCF7 cells incorporated BrdU. We took advantage of this distinct phenotype and carried out a functional 'rescue' experiment to confirm the specificity of the Nanog-shRNA effects. We cloned the HPCa5-*NANOGP8* cDNA into the pPyCAG expression plasmid [3] which, when transfected into MCF7 cells, produced NANOGP8 protein (fig. S14A). MCF7 cells transduced with LL3.7 or the two Nanog shRNA vectors were subsequently (24 h later) transfected with pPyCAG or pPyCAG-*NANOGP8* and, 48 h after transfection, cells were pulsed with BrdU. Immunostaining revealed that both Nanog shRNAs significantly downregulated the percentages of BrdU-positive cells and *NANOGP8*-cDNA fully 'rescued' (i.e., reversed) the Nanog shRNA phenotype but not the TRC-shRNA effect (Fig. 6C; fig. S14B). This was expected since Nanog shRNA targets the 3'-UTR whereas TRC-shRNA targets the coding region (Fig. 1A). Therefore, the *NANOGP8*-cDNA (encoded by pPyCAG-*NANOGP8*; fig. S14B) will still be degraded by TRC-shRNA but not by Nanog-shRNA. The functional rescue experiments strongly suggest that the loss-of-function phenotypes of Nanog shRNAs on cancer cell clonal/clonogenic growth and tumor development are direct and specific consequences of Nanog downregulation.

Nanog-shRNA transduced MCF7 cells also exhibited significantly decreased clonogenic growth (Fig. 6D-E) consistent with Nanog siRNA-mediated inhibition of sphere formation (fig. S2H). Upon passaging of the 1^{o} spheres, LL3.7-infected MCF7 cells showed robust 2^{o} sphere formation whereas the Nanog-shRNA 1^{o} spheres formed degenerate 2^{o} spheres that could not be further passaged (Fig. 6E and data not shown). The striking hollow spheres formed by Nanog-shRNA transduced MCF7 cells (Fig. 6E) suggest that Nanog knockdown

NIH-PA Author Manuscript

NIH-PA Author Manuscript

NIH-PA Author Manuscript

might be causing a differentiation phenotype. In support, the LL3.7-infected MCF7 tumors were comprised of characteristic undifferentiated, cytokeratin 18-positive carcinoma cells, many of which were proliferating as evidenced by positive Ki67 staining (Fig. 6F). In contrast, the two Nanog-shRNA infected MCF7 tumors demonstrated a more differentiated histology with numerous glandular-like structures exhibiting increased mucin production and fewer Ki67-positive cells (Fig. 6F).

DISCUSSION

In the present study, we have endeavored to systematically investigate the expression, origin, and functions of Nanog in tumor cells and we have made the following significant findings. *First*, multiple tumor cells in vitro and in vivo express *NANOGP8* mRNA as well as NANOG protein. *Second*, NANOG-positive cells are increased in prostate tumors compared to the benign tissues and, *NANOGP8* mRNA and NANOG protein seem to be enriched in the $CD44^{hi}$ PCa stem/progenitor cells. *Third*, most importantly, downregulation of Nanog inhibits tumor development of prostate, breast, and colon cancer cells. *Finally*, the tumor-inhibitory effects of Nanog knockdown are associated with an inhibition of cell proliferation, clonal expansion and clonogenic growth of tumor cells. Thus, Nanog expressed in human cancer cells is biologically functional in regulating tumor development.

Zhang et al. [31] has previously reported that several tumor cell lines express *NANOGP8*. We confirm and significantly extend these findings in a large panel of cancer cell lines and xenograft and primary HPCa samples. We further provide evidence that tumor cell-derived *NANOGP8* is biologically active in that its enforced expression could functionally rescue the proliferative defect caused by a 3'-UTR-targeting Nanog-shRNA. The present work, to our knowledge, represents the most comprehensive study on endogenous Nanog protein expression in cancer cells. Curiously, IF staining using the standard permeabilization protocol only identifies Nanog expression in a small population of cultured cells. Denaturation prior to immunolabeling, however, reveals NANOG expression as a hierarchy or gradient. Thus, a small percentage of cultured cancer cells seem to express high levels of NANOG that can be readily detected by regular staining protocol. A similar gradient in NANOG positivity has also been observed in PCa cells in situ, a heterogeneous Nanog expression pattern that is reminiscent of its expression pattern in ESCs [36]. Since most cultured N-tera cells readily reveal Nanog without requiring denaturation, the NANOG protein in cancer cells might be biochemically distinct and/or present in unique protein complexes.

The increased nuclear Nanog expression in a fraction of tumor cells raises the possibility that these cells might represent tumor stem/progenitor cells. In support, we have found evidence that both *NANOGP8* mRNA and NANOG protein are enriched in the $CD44^{hi}$ HPCa cell populations, which harbor colony- and tumor-initiating PCa stem/progenitor cells [24, 25, 34]. These observations are interesting in light of a recent report that suggests that cell surface CD44, upon binding to its ligand hyaluronan, may interact in the cytoplasm with NANOG in MCF7 cells to activate ABC transporter expression via a Stat3-dependent mechanism [37]. Indeed, we frequently observe a small fraction of cytoplasmically localized NANOG in cancer cells and, NANOG and CD44, though showing overall distinct subcellular localization, are sometimes observed adjacent to each other in the cytoplasm. Although normal prostate SCs are thought to localize mainly in the basal layer of the prostatic glands [38], NANOG-expressing PCa cells in tumor glands appear to localize in both basal and suprabasal layers. Preliminary observations show inverse nuclear NANOG and AR expression in a subset of PCa cells in situ (fig. S7B-C), consistent with the notion that NANOG-expressing PCa cells might be less differentiated cancer stem/progenitor cells. Further studies to validate the observed correlation between Nanog expression and PCa

NIH-PA Author Manuscript

NIH-PA Author Manuscript

NIH-PA Author Manuscript

stem/progenitor cells (e.g. $CD44^{+/high}$, $CD133^{+}$, $AR^{-/low}$) are currently ongoing. Regardless, our data show that NANOG-expressing cells are increased in PCa compared to corresponding benign tissues. Whether the abundance of NANOG-expressing cells correlates with tumor grade, stage, and propensity to disseminate will await further studies using a larger cohort of patient samples. Notably, through an unbiased prospective proteomic analysis, Alldridge et al. [8] reported that NANOG was overexpressed in primary breast cancers.

The most significant finding of the current study is that Nanog knockdown inhibits tumor development and this inhibitory effect has been observed in three different tumor systems. Since two Nanog-shRNAs targeting the 3'-UTR and one Nanog-shRNA targeting the coding region have all demonstrated inhibitory effects, the loss-of-function phenotypes are likely related to direct Nanog inhibition rather than to some off-target effects. In support, several different types of control vectors do not display tumor-inhibitory effects. Furthermore, in contrast to the reproducible tumor-inhibitory effects of Nanog knockdown, Oct4-shRNA shows inconsistent tumor-inhibitory effects. This latter observation is intriguing in that Nanog and Oct4 cooperate to regulate several hundred target genes and self-renewal process in ESCs [5, 6].

How might NANOG regulate tumor development? We have demonstrated that downregulation of Nanog is associated with decreased cancer cell proliferation both in vitro and in vivo. Furthermore, high NANOG-expressing cells are often found to be undergoing cell division. These observations are in accord with overexpressed Nanog being able to promote NIH3T3 cell proliferation [15]. The fact that Nanog downregulation inhibits *serial* clonal growth, sphere development, as well as serial tumor transplantations suggests that NANOG in tumor cells *might* enhance self-renewal. Alternatively, Nanog decrease may drive aberrant differentiation, such as that observed in Nanog-shRNA MCF7 tumors (this study). Further experiments are required to discriminate between relative contributions of altered proliferation, self-renewal and/or differentiation states, as well as associated perturbations in the cell cycle, in cancer cells exhibiting decreased NANOG expression.

Complementing the loss-of-function studies in tumors in the present study, we have found that ectopic expression of patient tumor-derived *NANOGP8* in the K14 cellular compartment in transgenic mice disrupts tissue homeostasis associated with hyperplasia, dysplasia, and abnormal differentiation (Badeaux et al; manuscript in preparation). Although we are still dissecting the detailed molecular mechanisms underlying these proliferation and differentiation defects caused by NANOG expression, the apparent dysplasia, hyperplasia, and abnormal differentiation, which are omnipresent histological traits of all benign tumors and cancers, strongly suggest that cancer cell NANOG could possess oncogenic potential.

In summary, our current study presents compelling experimental evidence that a variant of the ESC self-renewal gene *NANOG* also functions in human tumor development. The study also raises many critical questions, foremost among which are: How is *NANOGP8* transcriptionally activated and regulated in tumor cells? What are the NANOG-mediated signaling networks in tumor cells? Does NANOG expression promote tumor initiation and/or malignant progression? The answers to these important and interconnected questions, which we are actively pursuing, will help us better understand the functions of NANOG in regulating tumor development.

Supplementary Material

Refer to Web version on PubMed Central for supplementary material.

NIH-PA Author Manuscript

NIH-PA Author Manuscript

NIH-PA Author Manuscript

Acknowledgments

We are grateful to Dr. K. Kiguchi for confocal microscopy, K. Claypool for FACS, Dr. JJ Shen and MB Core for sequencing and qPCR, Nancy Otto and Histology Core for IHC, Drs. JJ Shen and M. Person and Proteomics Core for protein ID, S. Gaddis for sequence alignment, Animal Facility Core for tumor-related experiments, Drs. R. Fagin, S. Pickett, J. Waxman, and L. Dalton for primary HPCa samples, and other members of the Tang lab for support and helpful discussions. We also thank Dr. I. Chambers for the pPyCAG vector, and Dr. S. Orkin for critically reading the manuscript. This work was supported in part by grants from NIH (R01-AG023374, R01-ES015888, and R21-ES015893-01A1), American Cancer Society (RSG MGO-105961), Department of Defense (W81XWH-07-1-0616 and W81XWH-08-1-0472), Prostate Cancer Foundation, and Elsa Pardee Foundation (D.G.T) and by two Center Grants (CCSG-5 P30 CA166672 and ES07784). C. Jeter was supported in part by a postdoctoral fellowship from NIH and American Urological Association. G. Choy and D. Chandra were supported in part by a postdoctoral fellowship from DOD and an NIH K01 award, respectively. M. Badeaux and L. Patrawala were supported in part by predoctoral fellowships from NIEHS and DOD, respectively. We apologize to those colleagues whose work could not be cited due to stringent space limit.

REFERENCES

1. Visvader JE, Lindeman GJ. Cancer stem cells in solid tumours: accumulating evidence and unresolved questions. Nat Rev Cancer. 2008; 8:755–768. [PubMed: 18784658]
2. Vermeulen L, Todaro M, de Sousa Mello F, et al. Single-cell cloning of colon cancer stem cells reveals a multi-lineage differentiation capacity. Proc Natl Acad Sci U S A. 2008; 105:13427–13432. [PubMed: 18765800]
3. Chambers I, Colby D, Robertson M, et al. Functional expression cloning of Nanog, a pluripotency sustaining factor in embryonic stem cells. Cell. 2003; 113:643–655. [PubMed: 12787505]
4. Mitsui K, Tokuzawa Y, Itoh H, et al. The homeoprotein Nanog is required for maintenance of pluripotency in mouse epiblast and ES cells. Cell. 2003; 113:631–642. [PubMed: 12787504]
5. Boyer LA, Lee TI, Cole MF, et al. Core transcriptional regulatory circuitry in human embryonic stem cells. Cell. 2005; 122:947–956. [PubMed: 16153702]
6. Wang J, Rao S, Chu J, et al. A protein interaction network for pluripotency of embryonic stem cells. Nature. 2006; 444:364–368. [PubMed: 17093407]
7. Hoei-Hansen CE. Application of stem cell markers in search for neoplastic germ cells in dysgenetic gonads, extragonadal tumours, and in semen of infertile men. Cancer Treat Rev. 2008; 34:348–367. [PubMed: 18289797]
8. Alldridge L, Metodieva G, Greenwood C, et al. Proteome profiling of breast tumors by gel electrophoresis and nanoscale electrospray ionization mass spectrometry. J Proteome Res. 2008; 7:1458–1469. [PubMed: 18257521]
9. Ezeh UI, Turek PJ, Reijo RA, et al. Human embryonic stem cell genes OCT4, NANOG, STELLAR, and GDF3 are expressed in both seminoma and breast carcinoma. Cancer. 2005; 104:2255–2265. [PubMed: 16228988]
10. Ye F, Zhou C, Cheng Q, et al. Stem cell protein Nanog, nucleostemin and Musashi1 are highly expressed in malignant cervical epithelial cells. BMC Cancer. 2008; 8:108. [PubMed: 18419830]
11. Chiou SH, Yu CC, Huang CY, et al. Positive correlations of Oct-4 and Nanog in oral cancer stem-like cells and high-grade oral squamous cell carcinoma. Clin Cancer Res. 2008; 14:4085–4095. [PubMed: 18593985]
12. Bussolati B, Bruno S, Grange C, et al. Identification of a tumor-initiating stem cell population in human renal carcinomas. FASEB J. 2008; 22:3696–3675. [PubMed: 18614581]
13. Zhang S, Balch C, Chan M, et al. Identification and characterization of ovarian cancer-initiating cells from primary human tumors. Cancer Res. 2008; 68:4311–4320. [PubMed: 18519691]
14. Hochedlinger K, Yamada Y, Beard C, et al. Ectopic expression of Oct-4 blocks progenitor-cell differentiation and causes dysplasia in epithelial tissues. Cell. 2005; 121:465–477. [PubMed: 15882627]
15. Piestun D, Kochupurakkal BS, Jacob-Hirsch J, et al. Nanog transforms NIH3T3 cells and targets cell-type restricted genes. Biochem Biophys Res Commun. 2006; 343:279–285. [PubMed: 16540082]

NIH-PA Author Manuscript

NIH-PA Author Manuscript

NIH-PA Author Manuscript

16. Gibbs CP, Kukekov VG, Reith JD, et al. Stem-like cells in bone sarcomas: implications for tumorigenesis. Neoplasia. 2005; 7:967–976. [PubMed: 16331882]
17. Pain D, Chirn G, Strassel C, et al. Multiple retropseudogenes from pluripotent cell-specific gene expression indicates a potential signature for novel gene identification. J Biol Chem. 2005; 280:6265–6268. [PubMed: 15640145]
18. Liedtke S, Enczmann J, Waclawczyk S, et al. Oct4 and its pseudogenes confuse stem cell research. Cell Stem Cell. 2007; 1:364–366. [PubMed: 18371374]
19. Cantz T, Key G, Bleidissel M, et al. Absence of OCT4 expression in somatic tumor cell lines. STEM CELLS. 2008; 26:692–697. [PubMed: 18032701]
20. Lengner C, Camargo F, Hochedlinger K, et al. Oct4 expression is not required for mouse somatic stem cell self-renewal. Cell Stem Cell. 2007; 1:403–415. [PubMed: 18159219]
21. Chang C, Shieh G, Wu P, et al. Oct3/4 expression reflects tumor progression and regulates motility of bladder cancer cells. Cancer Res. 2008; 68:6281–6291. [PubMed: 18676852]
22. Hu T, Liu S, Breiter D, et al. Octamer 4 small interfering RNA results in cancer stem cell-like cell apoptosis. Cancer Res. 2008; 68:6533–6540. [PubMed: 18701476]
23. Patrawala L, Calhoun T, Schneider-Broussard R, et al. Side population (SP) is enriched in tumorigenic, stem-like cancer cells whereas ABCG2^{+} and ABCG2^{-} cancer cells are similarly tumorigenic. Cancer Res. 2005; 65:6207–6219. [PubMed: 16024622]
24. Patrawala L, Calhoun T, Schneider-Broussard R, et al. Highly purified CD44^{+} prostate cancer cells from xenograft human tumors are enriched in tumorigenic and metastatic progenitor cells. Oncogene. 2006; 25:1696–1708. [PubMed: 16449977]
25. Patrawala L, Calhoun-Davis T, Schneider-Broussard R, et al. Hierarchical organization of prostate cancer cells in xenograft tumors: the CD44$^{+}\alpha2\beta1^{+}$ cell population is enriched in tumor-initiating cells. Cancer Res. 2007; 67:6796–6805. [PubMed: 17638891]
26. Wang Y, Revelo MP, Sudilovsky D, et al. Development and characterization of efficient xenograft models for benign and malignant human prostate tissue. Prostate. 2005; 64:149–159. [PubMed: 15678503]
27. Zaehres H, Lensch MW, Daheron L, et al. High-efficiency RNA interference in human embryonic stem cells. STEM CELLS. 2005; 23:299–305. [PubMed: 15749924]
28. Hart AH, Hartley L, Ibrahim M, et al. Identification, cloning and expression analysis of the pluripotency promoting Nanog genes in mouse and human. Dev Dyn. 2004; 230:187–198. [PubMed: 15108323]
29. Booth HA, Holland PW. Eleven daughters of NANOG. Genomics. 2004; 84:229–238. [PubMed: 15233988]
30. Yeo S, Jeong S, Kim J, et al. Characterization of DNA methylation change in stem cell marker genes during differentiation of human embryonic stem cells. Biochem Biophys Res Commun. 2007; 359:536–542. [PubMed: 17548060]
31. Zhang J, Wang X, Li M, et al. NANOGP8 is a retrogene expressed in cancers. FEBS J. 2006; 273:1723–1730. [PubMed: 16623708]
32. Wang J, Levasseur DN, Orkin SH. Requirement of Nanog dimerization for stem cell self-renewal and pluripotency. Proc Natl Acad Sci U S A. 2008; 105:6326–6331. [PubMed: 18436640]
33. Tang DG, Patrawala L, Calhoun T, et al. Prostate cancer stem/progenitor cells: identification, characterization, and implications. Mol Carcinog. 2007; 46:1–14. [PubMed: 16921491]
34. Collins AT, Berry PA, Hyde C, et al. Prospective identification of tumorigenic prostate cancer stem cells. Cancer Res. 2005; 65:10946–10951. [PubMed: 16322242]
35. Li H, Chen X, Calhoun-Davis T, et al. PC3 human prostate carcinoma cell holoclones contain self-renewing tumor-initiating cells. Cancer Res. 2008; 68:1820–1825. [PubMed: 18339862]
36. Chambers I, Silva J, Colby D, et al. Nanog safeguards pluripotency and mediates germline development. Nature. 2007; 450:1230–1234. [PubMed: 18097409]
37. Bourguignon L, Peyrollier K, Xia W, et al. Hyaluronan-CD44 interaction activates stem cell marker Nanog, Stat-3-mediated MDR1 gene expression, and Ankyrin-regulated multidrug efflux in breast and ovarian tumor cells. J Biol Chem. 2008; 283:17635–17651. [PubMed: 18441325]

38. Lawson DA, Witte ON. Stem cells in prostate cancer initiation and progression. J Clin Invest. 2007; 117:2044–2050. [PubMed: 17671638]

NIH-PA Author Manuscript

NIH-PA Author Manuscript

NIH-PA Author Manuscript

NIH-PA Author Manuscript
NIH-PA Author Manuscript
NIH-PA Author Manuscript

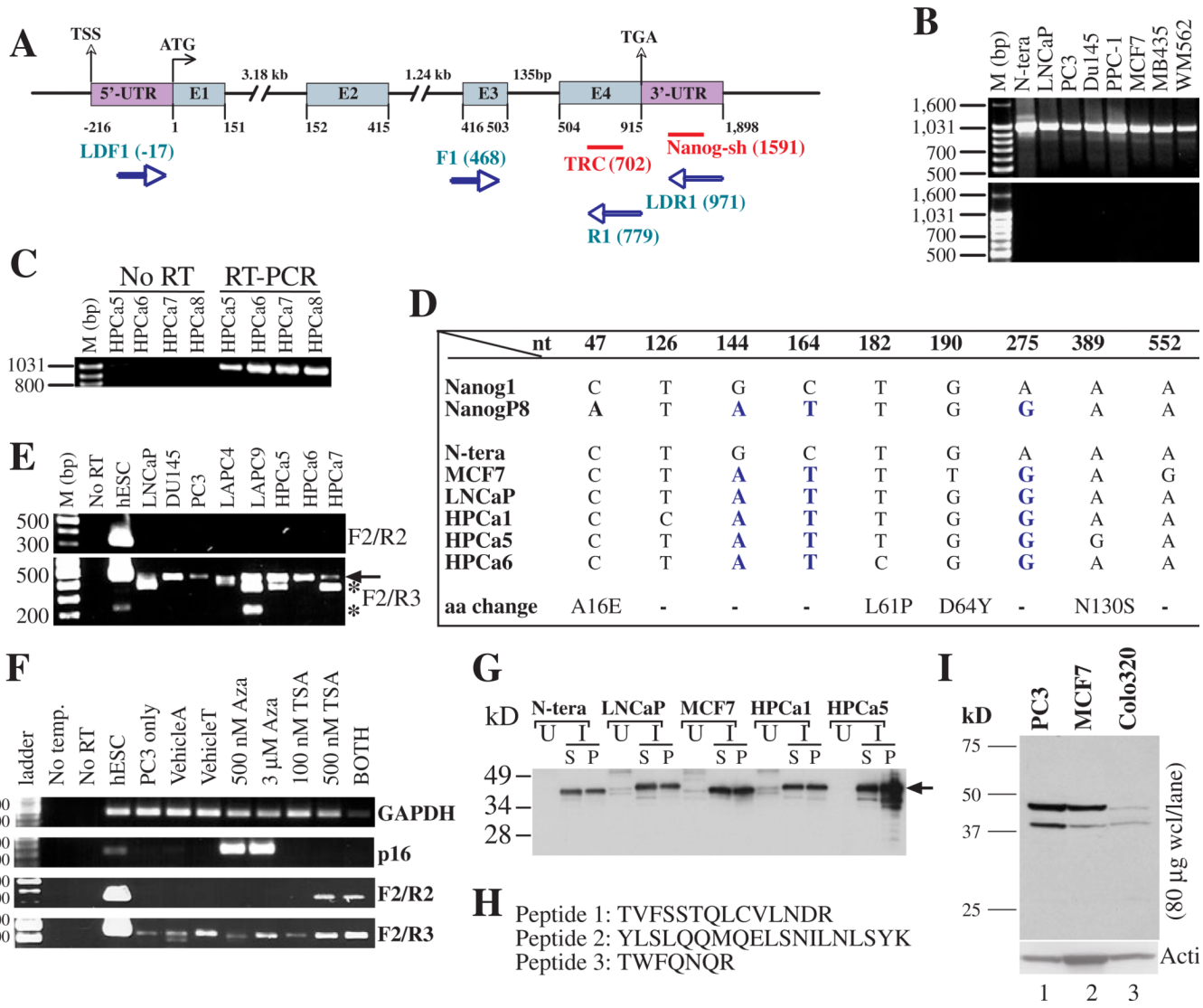

Figure 1. *NANOG* mRNA in cancer cells results from *NANOGP8*

(A) Schematic of human *NANOG1* gene structure. PCR primers and shRNA vector target locations are indicated in blue and red, respectively. Translational start ATG and stop TGA codons are indicated. E, exon; TSS, transcriptional start site; UTR, untranslated region.

(B-C) RT-PCR using LDF1-LDR1. 'No RT', no reverse transcription control. RNA/cDNA template was derived from cultured cancer cells (B) or primary HPCa samples (C).

(D) Sequencing analysis. Shown are the nucleotide (nt; and predicted aa) differences between cancer cell-derived *NANOG* and published *NANOG1* and *NANOGP8* sequences. The five conserved nts consistent with expression from the *NANOGP8* locus are indicated in blue. The single conserved predicted aa change is indicated in red.

(E) Differential RT-PCR. F2/R2 primers are specific for *NANOG1* whereas F2/R3 primers generate a 467-bp *NANOG1* product and a 446-bp *NANOGP8* product (arrow). The asterisks indicate two smaller amplicons.

(F) *NANOG1* in cancer cells is silenced. PC3 cells were treated (72 h) with AzaC and/or TSA (500 nM each), or vehicle. RT-PCR analysis of extracted RNA (non-treated hESC RNA for comparison) using the F2/R2 primers (*NANOG1* specific) vs. F2/R3 'universal'

NIH-PA Author Manuscript

NIH-PA Author Manuscript

NIH-PA Author Manuscript

NANOG primers. *p16 INK4a* (hypermethylated in PCa) amplification is used as AzaC control.

(G) Cancer cell *NANOGP8* cDNAs encode NANOG proteins that can be detected by an anti-NANOG1 antibody. Cancer cell *NANOGP8* cDNAs cloned in pET28b(−) were either uninduced (U) or induced (I) with IPTG and supernatant (S) or insoluble pellet (P) was used in Western blotting using the mAb. The arrow points to the ~42 kD NANOG band.

(H) Peptide sequences obtained by MALDI-TOF from MCF7 *NANOGP8* cDNA.

(I-J) Western blotting using whole cell lysate (WCL; I) or NE (J) and eBio mAb.

NIH-PA Author Manuscript
NIH-PA Author Manuscript
NIH-PA Author Manuscript

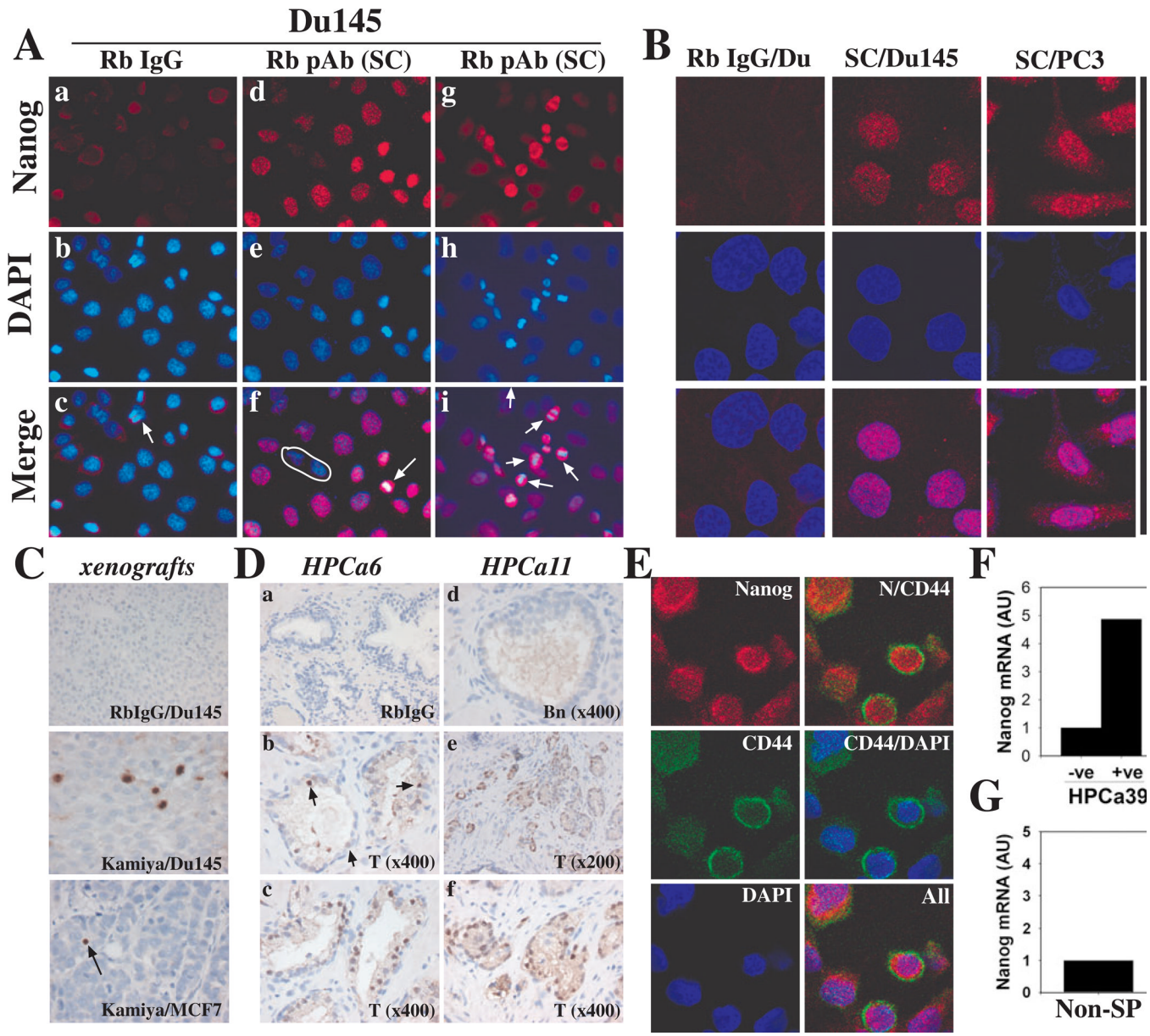

Figure 2. NANOG protein expression and enrichment in CD44^{hi} PCa cells

(A) Immunofluorescence (IF) staining of Du145 cells using rabbit (Rb) IgG (control; a-c) or the SC pAb to Nanog (d-i; arrows indicate dividing cells; circle demarcates non-expressors). Note that a dividing cell showed negative staining with Rb IgG (c, arrow).

(B) IF staining of cancer cells as in A and images analyzed under a confocal microscope. Shown are clusters of positive cells in N-tera, Du145, and PC3 cultures stained by the SC pAb.

(C) IHC staining of NANOG in Du145 and MCF7 tumor sections. Shown are a cluster of Nanog-positive cells in Du145 and a single positive cell in MCF7 (arrow) tumor sections.

(D) IHC staining of NANOG in HPCa sections using the Kamiya pAb. Staining with Rb IgG is shown as control. Arrows (b) point to scattered NANOG-positive cells. T, Tumor; Bn, Benign.

(E) Coordinate expression of NANOG and CD44 in Du145 cells. Shown are representative confocal images. N, NANOG.

NIH-PA Author Manuscript

NIH-PA Author Manuscript

NIH-PA Author Manuscript

(F-G) qRT-PCR analysis of *NANOGP8* mRNA expression in (F) $CD133^{+}$ (+ve)/$CD133^{-}$ (−ve) HPCa39 or $CD44^{+}CD133^{+}$ (+/+)/$CD44^{-}CD133^{-}$ (−/−) HPCa38 cells and (G) in MCF7 SP and non-SP cells.

NIH-PA Author Manuscript
NIH-PA Author Manuscript
NIH-PA Author Manuscript

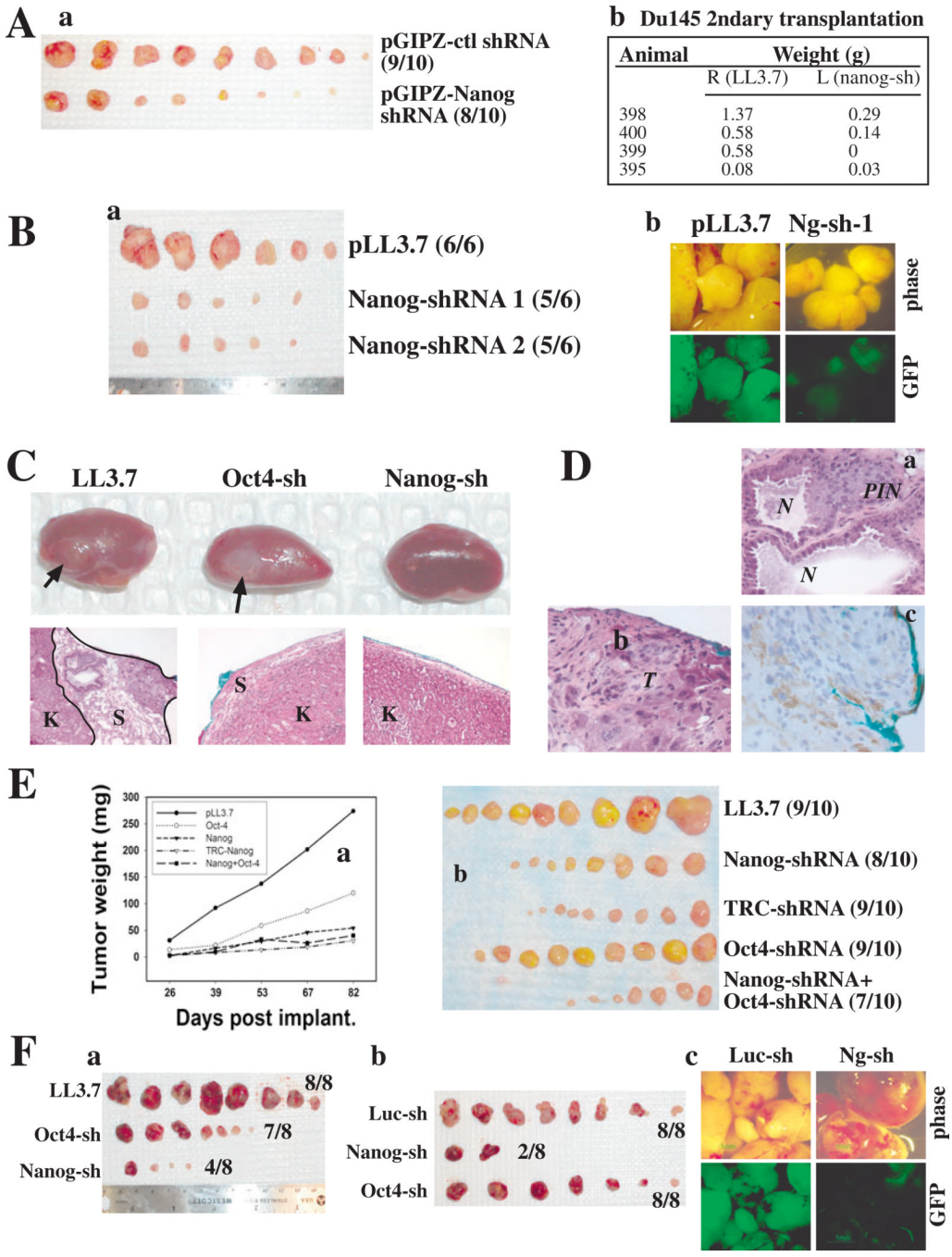

Figure 3. Downregulation of Nanog inhibits tumor development

(A) Nanog knockdown inhibits Du145 tumor development and serial transplantation. (a) Sphere-derived Du145 cells transduced with the indicated pGIPZ vectors at MOI of 10 were sorted 72 h later, and 25,000 cells injected s.c. in Matrigel into NOD/SCID mice. Tumors were harvested 63 d after injection (a) and tumor weights are indicated in Table 1. (b) 10,000 sorted GFP^+ tumor cells purified from 1^o tumors (Table 1) were used in 2^o transplantation.

(B) Nanog knockdown inhibits LAPC9 tumor development. (a) LAPC9 cells infected with the indicated vectors were sorted 72 h later and 1,000 GFP^+ tumor cells of each type were injected s.c in Matrigel into the male NOD/SCID mice supplemented with testosterone.

NIH-PA Author Manuscript

NIH-PA Author Manuscript

NIH-PA Author Manuscript

Tumors were harvested 61 d later. Nanog-sh 1 and 2 were two separate infections. Tumor weights are indicated in Table 1. (b) GFP images.

(C-D) Nanog knockdown inhibits HPCa tumor development. (C) Representative images of outgrowths (arrows; top) and corresponding histology (×100; bottom). (D) Enlarged images of outgrowth in LL3.7 recombinants (a and b; ×400) and IHC staining for human mitochondria (c). Note blue color indicates implantation site. K, mouse kidney; S, stroma; PIN, prostate intraepithelial neoplasia; N, normal glands; T, tumor.

(E) Nanog knockdown inhibits MCF7 tumor development. 100,000 MCF7 cells were transduced with the lentiviral constructs (MOI 20) and injected s.c. in Matrigel into female NOD/SCID mice supplemented with estrogen pellets. (a) Tumor growth curve (see SEP). (b) Tumor images.

(F) Nanog knockdown inhibits Colo320 tumor development. 250,000 Colo320 cells infected with the indicated lentiviruses (MOI 20) were injected in Matrigel s.c into the NOD/SCID mice. (a-b) Tumor images. Tumor weights are indicated in Table 1. (c) GFP images

NIH-PA Author Manuscript
NIH-PA Author Manuscript
NIH-PA Author Manuscript

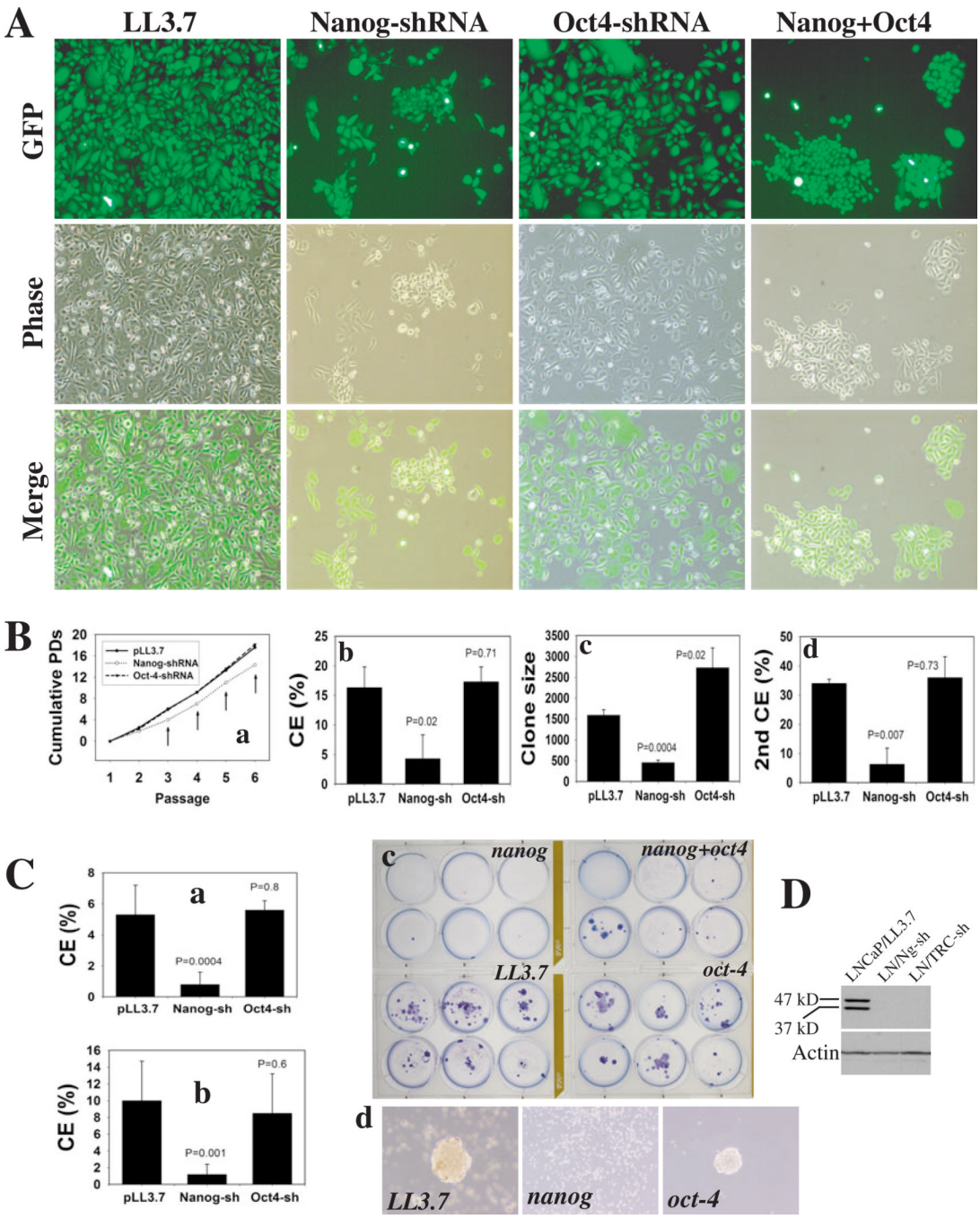

Figure 4. Nanog downregulation restricts clonal and clonogenic growth of PCa cells

(A) PC3 cells infected with the indicated lentiviral vectors (MOI 25) were dissociated and replated, 72 h later, at clonal density in a 6-well plate (100 cells/well). Images 12 d post-plating (×200).

(B) PC3 cells infected with the indicated vectors (above) were serially passaged and cumulative PDs determined (a). Arrows, $P<0.05$. (b) 1^o clonal efficiency (CE): 100 infected PC3 cells were plated per well in a 6-well plate; clones were counted 10 d or (c) 17 d after plating. (d) 2^o clonal analysis: 1^o clones were cloned out using a cloning ring and replated at 100 cell/well; 2^o clones were counted at 10 d. For b-d, data for each condition were derived from at least 6 samples (mean ± S.D).

NIH-PA Author Manuscript

NIH-PA Author Manuscript

NIH-PA Author Manuscript

(C) 100 infected LNCaP cells (transduced as described above) were plated for CE and clones scored at (a) 14 d or (b) 37 d post plating. (c) Giemsa staining of clones at 37 d. (d) LNCaP 2^o clonogenicity: 1,000 infected LNCaP cells were plated on 1% agarose, and, 15 d later, 1^o spheres were harvested, dissociated with trypsin and replated.
(D) Western blotting (60 μg wcl/lane; eBio mAb) of LNCaP cells infected with LL3.7, Nanog- or TRC-shRNAs (72 h post infection).

NIH-PA Author Manuscript
NIH-PA Author Manuscript
NIH-PA Author Manuscript

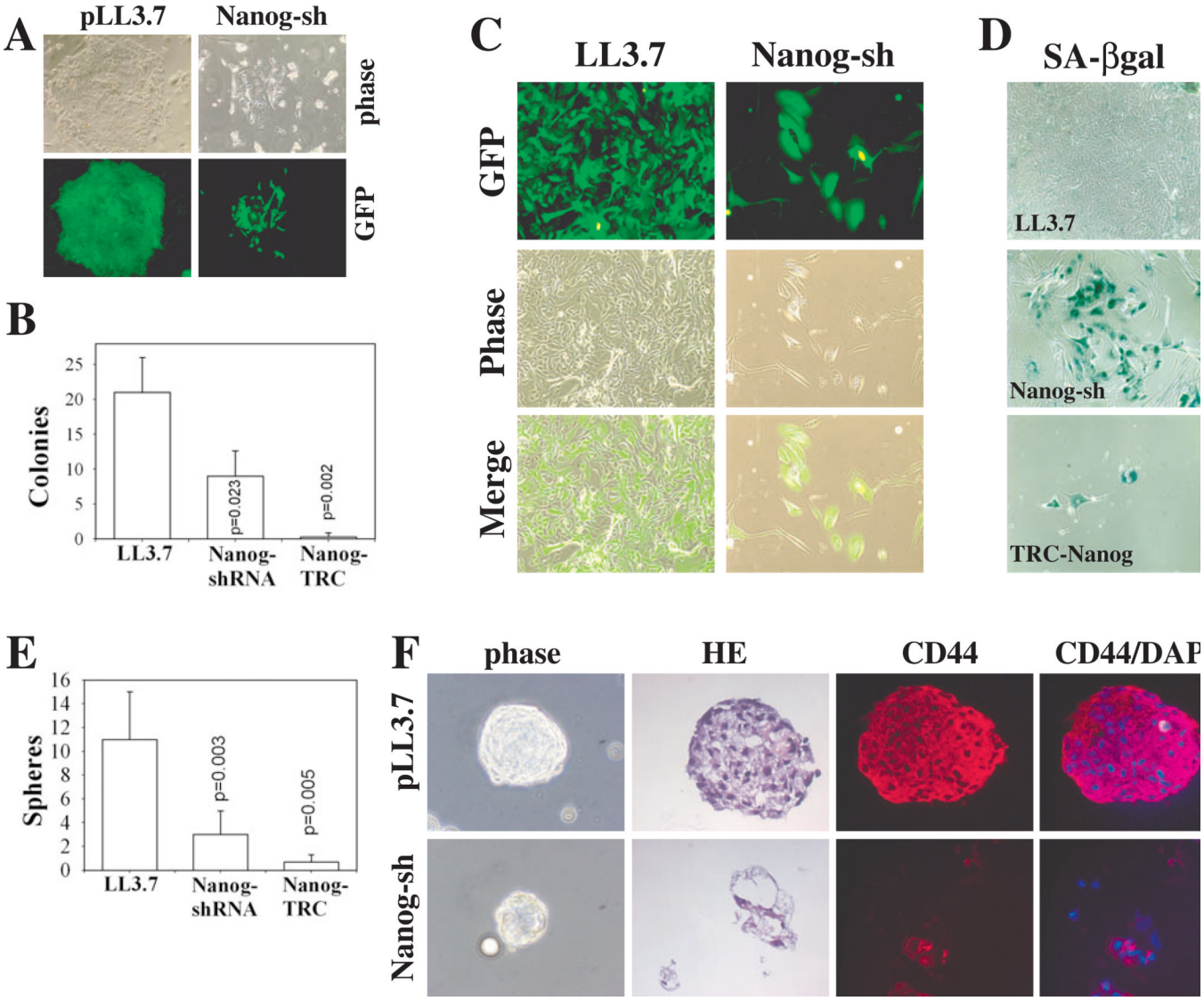

Figure 5. Nanog downregulation restricts clonal and clonogenic growth of primary HPCa cells

(A-D) Nanog knockdown inhibits clonal expansion of HPCa22 cells. Freshly purified HPCa22 cells were infected overnight with indicated lentivirus and plated (n = 3) at 10,000 cells/well on mitomycin C-treated Swiss 3T3 fibroblast feeders. (A) Representative images of clones in C (×100). (B) Holoclones were enumerated 16 d after plating; results represent the mean ± S.D. (C) 2^o clonal analyses: HPCa22 1^o clones were dissociated and replated on fibroblasts and, (D) 3 weeks later, cells were stained for SA-βgal (×100).

(E-F) Nanog knockdown inhibits sphere formation of HPCa22 cells. (E) Transduced HPCa22 cells (above), were plated (n = 3) at 25,000 cells/well (in 6-well plate) on agarose. Spheres were enumerated 16 d after plating and the results represent the mean ± S.D. (F) Representative images (×100) of OCT-embedded spheres; hematoxylin and eosin (HE) and IF staining for CD44 (red) and DNA (DAPI-blue).

NIH-PA Author Manuscript
NIH-PA Author Manuscript
NIH-PA Author Manuscript

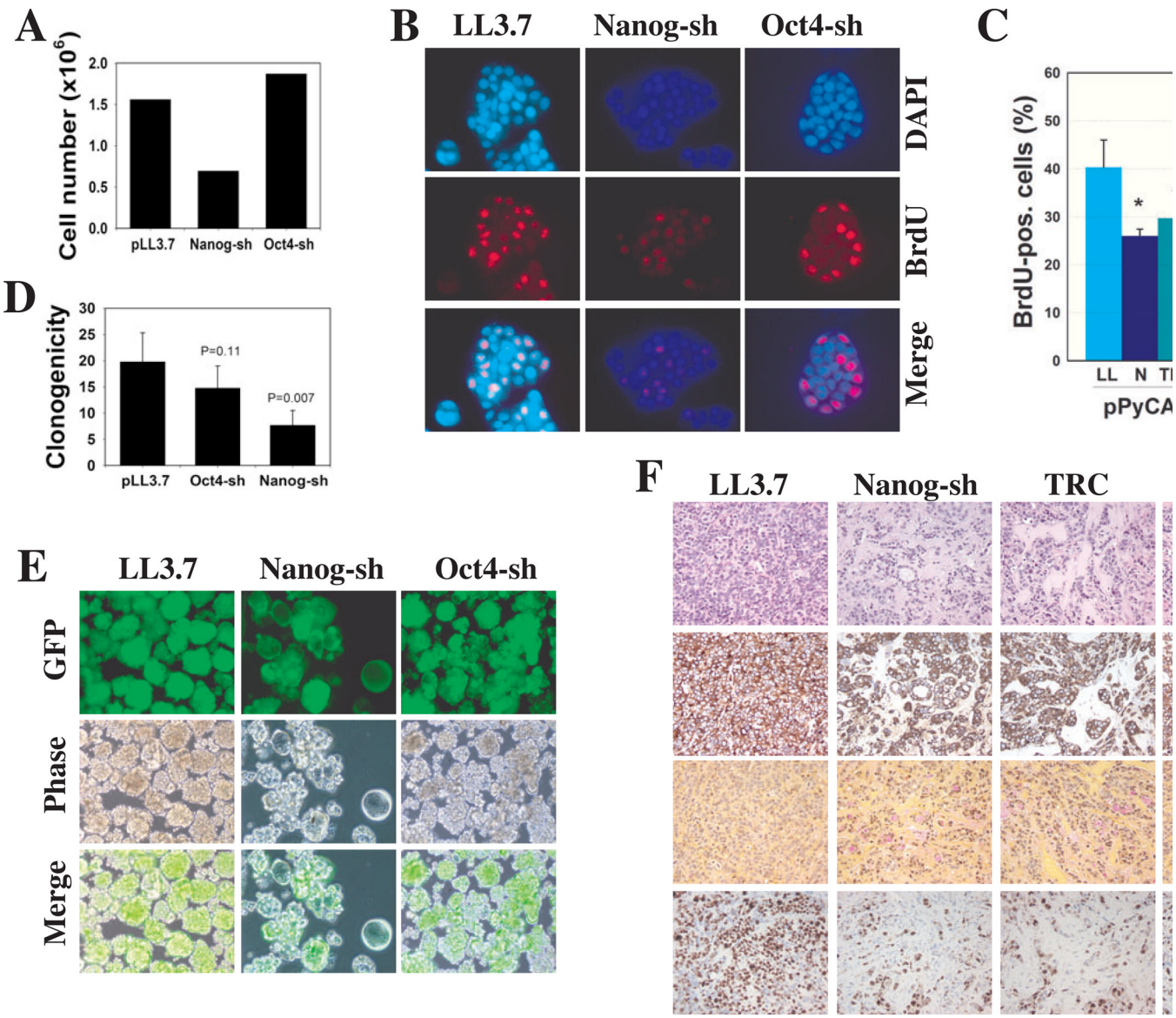

Figure 6. Nanog knockdown inhibits MCF7 cell clonogenic growth, reduces proliferation and alters differentiation

(A) MCF7 clonal growth. 100 MCF7 cells infected with the indicated vectors were plated (n = 3) in 6-well plates. 21 d post-plating, cells were trypsinized, pooled and counted.

(B) BrdU incorporation assays. MCF7 cells infected with the indicated lentiviruses were cultured overnight on glass coverslips and pulsed with 5 μM BrdU for 4 h. Fixed cells were processed for BrdU immunostaining (red), markedly reduced in Nanog-shRNA transduced cells.

(C) Functional 'rescue' experiments. MCF7 cells were infected with the indicated vectors (LL, LL3.7; N, Nanog-shRNA; TRC, TRC-shRNA; MOI 20) and 24 h later, transfected with either pPyCAG or pPyCAG-PN8 (i.e., *NANOGP8*). 48-h later cells were pulsed with BrdU (4 h) and processed for BrdU staining. A total of 500–1,000 cells were counted by three individuals and the bars represent the mean ± S.D. *P < 0.05 between the two conditions.

(D) 2^{o} MCF7 clonogenic growth. 1,000 MCF7 cells were plated (n = 3) on agarose, and spheres were scored 10 d post-plating.

NIH-PA Author Manuscript

NIH-PA Author Manuscript

NIH-PA Author Manuscript

(E) 2^{o} sphere images. 1^{o} spheres were harvested (10 d after infection) and replated. Shown are representative images one month after replating.
(F) Tumors derived from Nanog-shRNA and TRC-Nanog shRNA-infected MCF7 cells appeared more differentiated (ductal structures and increased mucin) and exhibit lower proliferation (Ki67) than the control tumors. 5-μm serial sections were stained for HE or the molecules indicated on the right (×200).

NIH-PA Author Manuscript
NIH-PA Author Manuscript
NIH-PA Author Manuscript

Table 1

Nanog knockdown inhibits tumor development

Experiments[a]	Tumor incidence[b]	Weight (g)[c]	P values[d]
Du145 (75k/injection; 56d)			
pLL3.7	8/8	0.25 ± 0.05	
Nanog-shRNA	8/8	0.13 ± 0.07	0.02
Du145 (10k/injection)			
pLL3.7 (62d)	7/8	0.71 ± 0.45	
Nanog-shRNA (62d)	7/8	0.32 ± 0.18	0.045
Du145 (25k/injection; 63d)			
pGIPZ-control	9/10	0.50 ± 0.32	
pGIPZ-Nanog	6/10*	0.22 ± 0.27	0.038
LAPC9 (1k/inj; 60d)			
pLL3.7	6/6	1.03 ± 0.25	
Nanog-shRNA 1*	5/6	0.04 ± 0.03	0.04
Nanog-shRNA 2*	5/6	0.076 ± 0.07	0.04
LAPC4 (150k/inj; 67d)			
pLL3.7	6/6	0.08 ± 0.05	
Nanog-shRNA	5/6	0.02 ± 0.008	0.017
TRC Nanog-shRNA	2/6**	0.02 ± 0.001	0.01
HPCa18 (100k/TR; 150d)#			
pLL3.7	2/2	N/A	
Nanog-shRNA	0/2	N/A	
MCF7 (100k/injection; 97d)			
pLL3.7	9/10	0.45 ± 0.13	
Nanog-shRNA	8/10	0.09 ± 0.02	0.028
TRC Nanog-shRNA	9/10	0.05 ± 0.016	0.012
Oct4-shRNA	9/10	0.20 ± 0.03	0.1
Nanog-shRNA + Oct4-hRNA	7/10	0.06 ± 0.014	0.029
Colo320 (25k/injection; 35d)			
pLL3.7	5/5	0.11 ± 0.07	
Nanog-shRNA	3/5*	0.076 ± 0.02	0.042
Colo320 (250k/injection; 35d)			
pLL3.7	8/8	0.82 ± 0.38	
Nanog-shRNA	4/8**	0.058 ± 0.008	0.003
Oct4-shRNA	7/8	0.26 ± 0.19	0.006
Colo320 (250k/injection; 34d)			
pLL3.7-luciferase	8/8	0.77 ± 0.48	
Nanog-shRNA	2/8**	0.67 ± 0.17	0.79
Oct4-shRNA	8/8	0.52 ± 0.41	0.29

[a] Cultured cancer cells or xenograft-purified cells were infected with the indicated lentiviral vectors at an MOI of 20.24–48 h after infection, different numbers (k) of cells were injected subcutaneously in Matrigel (50%) into NOD/SCID mice. Termination time in days (d) is indicated in parentheses.

The asterisks (*) indicate two independent infections of LAPC9 cells in the same experiment.

For HPCa18 (#), 100,000 infected cells were recombined with 200,000 rUGM cells and transplanted under the kidney capsule and the tissue recombinants (TR) were harvested 5 months later.

[b] Number of tumors developed/number of injections.

[*] $P < 0.05$;

[**] $P < 0.01$ (χ^2 test).

[c] Mean ± S.D. N/A, not available.

[d] Statistical comparisons (Student *t*-test) for tumor weights were made with the control (pLL3.7, pGIPZ-control or pLL3.7-luciferase) group.

NIH-PA Author Manuscript NIH-PA Author Manuscript NIH-PA Author Manuscript